2nd International Conference on System-Integrated Intelligence: Challenges for Product and Production Engineering

Adaptive controller algorithm for 2-DOF humanoid robot arm

Adam Tan Mohd Amin[a]*, Abdul Hakim Ab Rahim[a], Cheng Yee Low[a,b]

[a]*Humanoid Robot and Bio-Sensing Center, Faculty of Mechanical Engineering, Universiti Teknologi MARA, 40450 Shah Alam,Malaysia*
[b]*Brain and Neuroscience Communities of Research, Universiti Teknologi MARA, 40450 Shah Alam, Malaysia*

Abstract

A computational model of human motor control for a nonlinear 2 degrees-of-freedom (DOF) robot arm to mimic humanlike behavior is developed and presented in this paper. The model is based on a simple mathematical model of a 2-segment compound pendulum which mimics the human upper arm and forearm. Using the Lagrangian and Euler-Lagrange equations, the 2-DOF dynamic equations were successfully derived and solved using Euler's method. Two types of controllers; a feedback Proportional-Derivative (PD) controller and a feedforward controller, were combined into the model. The algorithm exhibited learning of the necessary torque required in performing the desired Position Control via Specific Trajectory (PCST) rehabilitative task via feedback control and using it as the feedforward torque in subsequent trial motions. After 30 trials, the mean absolute error with respect to the desired motion of the upper arm, showed a decrease from 0.09533 to 0.005859, and the forearm motion from 0.3526 to 0.006138. This decrement trend in mean absolute errorwith increase in number of trials is consistent with the adaptive control strategy of the human arm known as the Feedback Error Learning (FEL) strategy.

1. Introduction

Robotic rehabilitation is an area that is vastly being developed at present. It includes the development of robotic therapies with the use of robots as therapy aids, instead of solely as assistive devices used by therapists. Studies have

_____

* Corresponding author. Tel.: +6019-6019509; fax: +603-55435160.
*E-mail address:*adamtan@salam.uitm.edu.my

proved that the presence of robots during rehabilitation can greatly improve the movement performance in patients suffering impairments either due to neurological or orthopedic maladies. It is also proven that automated robot-assisted and task-oriented repetitive movements can also improve muscular strength and movement coordination on these patients [1-3].

At present, the problem faced by using manually-assisted movement exercises such as therapists showed major limitations. Usually, these physiotherapy training sessions are considered labor-intensive and the training duration is usually limited either by personnel shortages or therapist fatigue during the sessions [4-5]. These indirectly affect the sessions to become shorter than required to gain an optimal outcome. Other than that, since the sessions are conducted by a therapist worker, repeatability accuracy and objective measures of patients are often questionable.

On the other hand, with automated therapy such as robot assisted arm training, the duration and number of training sessions can be optimized while reducing the number of therapists required per patient. Long term automated therapy appears to be the only way to make the intensive arm training affordable for clinical use. In the development of robot assisted arm training, the first step is to actually develop an algorithm that exhibits humanlike behavior so that it can be implemented to the rehabilitation robot.

2. Methodology

The development of the adaptive controller algorithm was conducted in 3 phases. The initial phase of the study involves *deriving and solving the 2-DOF dynamic equation*. In this phase, the basic elements of the overall algorithm are constructed by the derivation of the 2-DOF dynamic equations. The equations, based on a simple mathematical model of a 2-segment compound pendulum that mimics a human upper arm and forearm, as well as using the *Lagrangian* and *Euler-Lagrange equations* [6-8], are presented. The Euler's method is chosen for its robustness [9] to solve the derived dynamic equations. This phase of study is essential because the adaptive control strategies that are thought to be executed by humans are investigated based on these obtained dynamic equations and solutions.

The algorithm is expanded to the second phase which is *modelling humanlike properties* into the system. This is achieved by adding two types of controllers; first is the conventional feedback *Proportional-Derivative* (PD) controller [10], and later, combining it with a second controller known as the feed forward controller [11]. The humanlike properties are modelled using this algorithm and certain simulation tasks are assigned in order to test them. The task that was conducted is similar to a rehabilitation task for common patients [1-2]. It includes *Position Control via Specific Trajectory* (PCST) task, where the 2-DOF arm model is assigned to move from a certain position to another via a specified smooth trajectory pathway [12-13].

Finally, the *evaluation of the overall results* obtained is presented and discussed thoroughly in terms of its achievement and shortcomings as well as providing recommendations for future study.

2.1. Deriving and solving 2-DOF dynamic equation

The dynamic equation of a 2-DOF arm model can be derived using the Free Body Diagram (FBD) analysis of a simple double segment compound pendulum, a pendulum with another similar pendulum attached to its end as shown in Fig. 1.
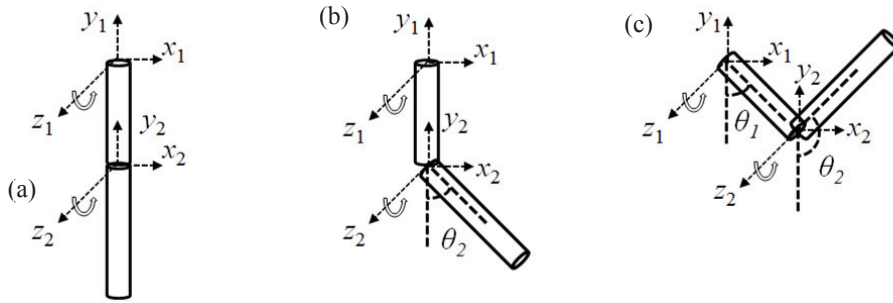
Fig. 1. Double segment compound pendulum on a 3-D axis which is analogous to a human upper arm and forearm; (a) at rest position, θ1 = θ2 = 0°; (b) the forearm rotates about the z-axis across the x-y plane with θ2 = 45°, while the upper arm remains at rest; (c) both the upper arm and forearm rotates about the z-axis across the x-y plane with θ1 =45° and θ2 = 135°.

It is a simple physical system that exhibits rich dynamic behavior with a strong sensitivity given its initial conditions [14]. The dynamics of a double segment compound pendulum is governed by a set of coupled nonlinear ordinary different equations, attainable by using the Lagrangian, as well as the Euler-Lagrange equation.

The *center of mass* of each limb (upper arm and forearm) depends on the mass distribution of each segment and since in a compound pendulum, the mass is assumed to be evenly distributed, the position of the center of mass is located at each midpoint of the limb. Therefore, by manipulating the *moment of inertia* [15-16] at that location, and using the *parallel axes theorem* [17] towards about the *z*-axis, the mathematical models for each limb can be derived to become as follows:

$$x_1 = 0.5 \, l_1 \sin(\theta_1)$$

$$y_1 = -0.5 \, l_1 \cos(\theta_1) \tag{1}$$

$$x_2 = l_1 \sin(\theta_1) + 0.5 \, l_2 \sin(\theta_2)$$

$$y_2 = - l_1 \cos(\theta_1) - 0.5 \, l_2 \cos(\theta_2) \tag{2}$$

Equations (1) and (2) refer to the mathematical model for both, the *x*- and *y*-coordinates of the upper arm and forearm respectively.

The Lagrangian, *L*, of a dynamical system is a function that summarizes the dynamics of a particular system. Its natural form is defined as the total kinetic energy, *T*, of the system minus its total potential energy, *V*,[4-6] as shown in equation (3). The total kinetic energy, which is the sum of both linear, T_E and rotational, T_R kinetic energy, can be derived using the formula shown in equation (4), whilst the equation for the total potential energy, *V* is shown in equation (5).

$$L = T - V \tag{3}$$

$$T = T_E + T_R$$
$$= \left(\frac{1}{2} \cdot m_1 \cdot v_1^2 + \frac{1}{2} \cdot m_2 \cdot v_2^2 \right) + \left(\frac{1}{2} \cdot I_1 \cdot \dot{\theta}_1^2 + \frac{1}{2} \cdot I_2 \cdot \dot{\theta}_2^2 \right) \tag{4}$$

$$V = m_1 g \, y_1 + m_2 \, g \, y_2 \tag{5}$$

If the Lagrangian of a system is known, then the system's equations of motion may be obtained by a direct substitution of the expression for the Lagrangian into the Euler-Lagrange equation [6-8], which is a set of

differential equations whose solutions describe the evolution of the physical system, given a range of time. Equation (6) shows the formula for the Euler-Lagrange equation:

$$\frac{\delta L}{\delta \theta_1} - \frac{d}{dt}\left(\frac{\delta L}{\delta \dot{\theta}_1}\right) = 0 \tag{6}$$

Using the Euler-Lagrange equation for both upper arm and forearm, the dynamic equations for both limbs can be obtained, as shown in equation (7) and (8) respectively below:

$$\left(\frac{m_1}{3} + m_2\right) \cdot l_1 \cdot \ddot{\theta}_1 = -\frac{1}{2} \cdot m_2 \cdot l_2 \cdot \ddot{\theta}_2 \cdot \cos(\theta_1 - \theta_2) - \frac{1}{2} \cdot m_2 \cdot l_2 \cdot \dot{\theta}_2^2 \cdot \sin(\theta_1 - \theta_2) - \left(\frac{m_1}{2} + m_2\right) \cdot g \cdot \sin\theta_1 \tag{7}$$

$$\frac{13}{12} \cdot m_2 \cdot l_2 \cdot \ddot{\theta}_2 = -\frac{1}{2} \cdot m_2 \cdot l_1 \cdot \ddot{\theta}_1 \cdot \cos(\theta_1 - \theta_2) + \frac{1}{2} \cdot m_2 \cdot l_1 \cdot \dot{\theta}_1^2 \cdot \sin(\theta_1 - \theta_2) - \frac{m_2}{2} \cdot g \cdot \sin\theta_2 \tag{8}$$

In order to obtain the angular displacement trajectory for both upper arm and forearm, the derived dynamic equations for $\ddot{\theta}_1$ and $\ddot{\theta}_2$ need to be solved respectively. These equations can be solved by using a range of numerical methods. However, the Euler's method, as shown in equation (9) is chosen in this algorithm due to its robustness when writing the MATLAB® codes and only compensates a minimal tolerable error when solving the equations [9], compared to other numerical techniques.

$$\theta(t+1) = \theta(t) + \dot{\theta}(t) \cdot \text{dt} \tag{9}$$

2.2. Modelling humanlike properties

A particular control strategy that humans exert when carrying out a task is known as the Feedback Error Learning (FEL) strategy. This can be achieved by expanding the dynamic equations that were derived earlier with a set of controllers, and introducing a task into the algorithm to test them.

Usually, for a physically impaired patient as a result from stroke or other spinal cord injuries that affects a person's psychomotor abilities, the rehabilitation treatment process would require the patient to move the affected limb repetitively, in order to reactivate the affected muscles [1-3, 18]. In this study, mimicking the humanlike behavior when moving the arm from one position to another (e.g. during rehabilitation task), a *Position Control via Specific Trajectory* (PCST) task is introduced. The 2-DOF system will receive the desired initial, θ_i and final position, θ_f for both upper arm and forearm from the user or therapist, and will carry out repetitive tasks via a smooth trajectory, based on the equation shown in equation (10) below [19]:

$$\theta(t) = \theta_i + \left(\theta_f - \theta_i\right) \cdot \left(10 \cdot t^3 - 15 \cdot t^4 + 6 \cdot t^5\right) \tag{10}$$

Executing the algorithm in MATLAB® software, estimated anthropometric data of the human arm are necessary to generalize the calculations and findings. In this study, the required length and mass data for the human upper arm and forearm are obtained from current literatures [20], and are shown in Table 1 below:

Table 1. Anthropometric data of human upper arm and forearm, obtained from literatures.

Arm Segment	Length (m)	Mass (kg)
Upper arm	.290	1.794
Forearm	0.373	1.354

2.3. PCST task with PD feedback controller

Computing a motion function which causes a system to move from one position to another via a smooth minimum jerk trajectory is known as trajectory generation and control. A trajectory is defined not only by the desired destination for the system to move to, but also by continuous intermediate locations through which the system must pass, en route to the destination.

Executing the PCST task, a feedback controller is added into the algorithm, where the obtained trajectory is then compared with the desired trajectory (set by PCST), and the absolute error is computed and fed back to the system. The required torqueto compensate this error is generated by a conventional *Proportional-Derivative* (PD) feedback controller, separately for both upper arm and forearm limbs as shown in equations (11) and (12) respectively.

$$\left(\frac{m_1}{3}+m_2\right)\cdot l_1\cdot\ddot{\theta}_1 = -\frac{1}{2}\cdot m_2\cdot l_2\cdot\ddot{\theta}_2\cdot\cos\left(\theta_1-\theta_2\right)-\frac{1}{2}\cdot m_2\cdot l_2\cdot\dot{\theta}_2^{\;2}\cdot\sin\left(\theta_1-\theta_2\right)-\left(\frac{m_1}{2}+m_2\right)\cdot g\cdot\sin\theta_1-FB_1 \qquad (11)$$

$$\frac{13}{12}\cdot m_2\cdot l_2\cdot\ddot{\theta}_2 = -\frac{1}{2}\cdot m_2\cdot l_1\cdot\ddot{\theta}_1\cdot\cos\left(\theta_1-\theta_2\right)+\frac{1}{2}\cdot m_2\cdot l_1\cdot\dot{\theta}_1^{\;2}\cdot\sin\left(\theta_1-\theta_2\right)-\frac{m_2}{2}\cdot g\cdot\sin\theta_2-FB_2 \qquad (12)$$

Based on these two equations, *FB* is thepiecewise torque produced by the controller to compensate for the error produced during each trial, and is governed by equation (13) where*e*(*t*) is the error generated when the obtained trajectory is compared with the desired trajectory; *P* and *D,* are the control gain parameters for the *Proportional* and *Derivative* terms respectively, for each degree of freedom. Fig. 2 below illustrates the block diagram representation for this PD feedback controller that is added to the nonlinear 2-DOF arm model system.

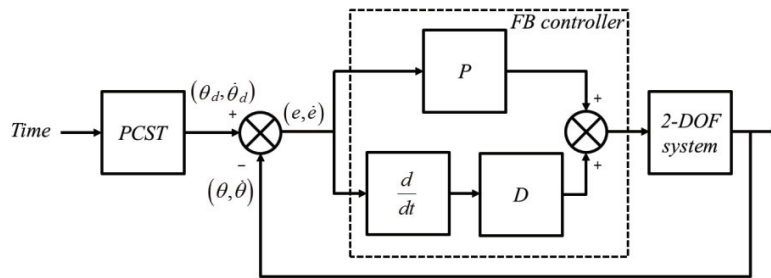$$FB(t) = P\cdot e(t) + D\cdot\dot{e}(t) \qquad (13)$$

Fig. 2. The block diagram representation of the Proportional-Derivative (PD) feedback controller scheme. PCST is the designated motion planner that provides the desired position and trajectory pathway for the system to achieve.

Using this PD feedback controller, the 2-DOF system is assigned with an initial position at 0° and final position 180°. The results are presented and discussed in the *Computational Results and Discussion* section.

2.4. PCST with PD feedback and feedforward controller

The performance of the algorithm is further enhanced by adding a feedforward controller, in which, when the movement is repeated during the PCST task, the controller gradually learns the necessary torque that is required to perform the task. During each trial, the torque that is produced by the feedback controller is used as feedforward torque in subsequent movements. The algorithm that is used as feedforward controller for both upper arm and forearm are described by equations (14)& (15) below:

$$\left(\frac{m_1}{3}+m_2\right)\cdot l_1\cdot\ddot{\theta}_1=-\frac{1}{2}\cdot m_2\cdot l_2\cdot\ddot{\theta}_2\cdot\cos\left(\theta_1-\theta_2\right)-\frac{1}{2}\cdot m_2\cdot l_2\cdot\dot{\theta}_2^{\;2}\cdot\sin\left(\theta_1-\theta_2\right)-\left(\frac{m_1}{2}+m_2\right)\cdot g\cdot\sin\theta_1-FB_1-FF_1 \quad (14)$$

$$\frac{13}{12}\cdot m_2\cdot l_2\cdot\ddot{\theta}_2=-\frac{1}{2}\cdot m_2\cdot l_1\cdot\ddot{\theta}_1\cdot\cos\left(\theta_1-\theta_2\right)+\frac{1}{2}\cdot m_2\cdot l_1\cdot\dot{\theta}_1^{\;2}\cdot\sin\left(\theta_1-\theta_2\right)-\frac{m_2}{2}\cdot g\cdot\sin\theta_2-FB_2-FF_2 \quad (15)$$

Based on equations (14)& (15), *FF* is the feedforward torque that will be used in performing the task in the subsequent $(t+1)$ trial, that is obtained from the torque by the feedback controller *FB*, at trial *t*. The feedforward controller gain that determines the amount of feedback torque to be used as feedforward is represented by the symbol,α, shown in equation (16). Fig. 3 shows the overall block diagram representation of the adaptive controller.

$$FF(t+1)=FF(t)+\alpha\cdot FB(t) \quad (16)$$

A similar instruction is assigned to the system using this adaptive controller algorithm, where the initial position of the 2-DOF system is set at 0° and final position at 180°. The results are also presented and discussed in the *Computational Results and Discussion* section. This controller combination between feedback and feedforward control is also known as a non-parametric adaptive controller [21], which is used to emulate the Feedback Error Learning (FEL) control strategy that is exhibited by humans.
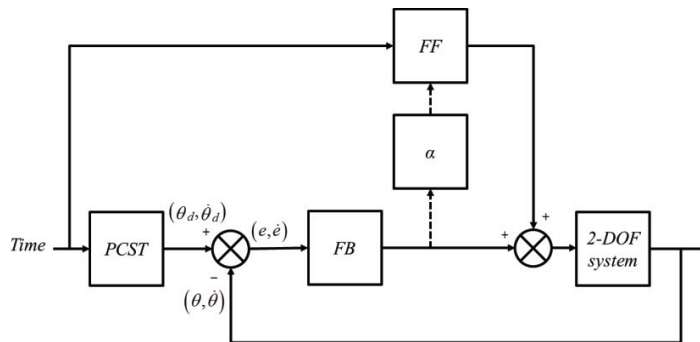

Fig. 3. The block diagram representation of the adaptive controller scheme which is a combination between feedback and feedforward controller, thus exhibiting the Feedback Error Learning (FEL) control strategy.

3. Computational Results and Discussion

3.1. PCST task with PD feedback controller

Fig. 4below illustrates the computational results from the simulation done in MATLAB® when executing the algorithm using only the PD feedback controller:
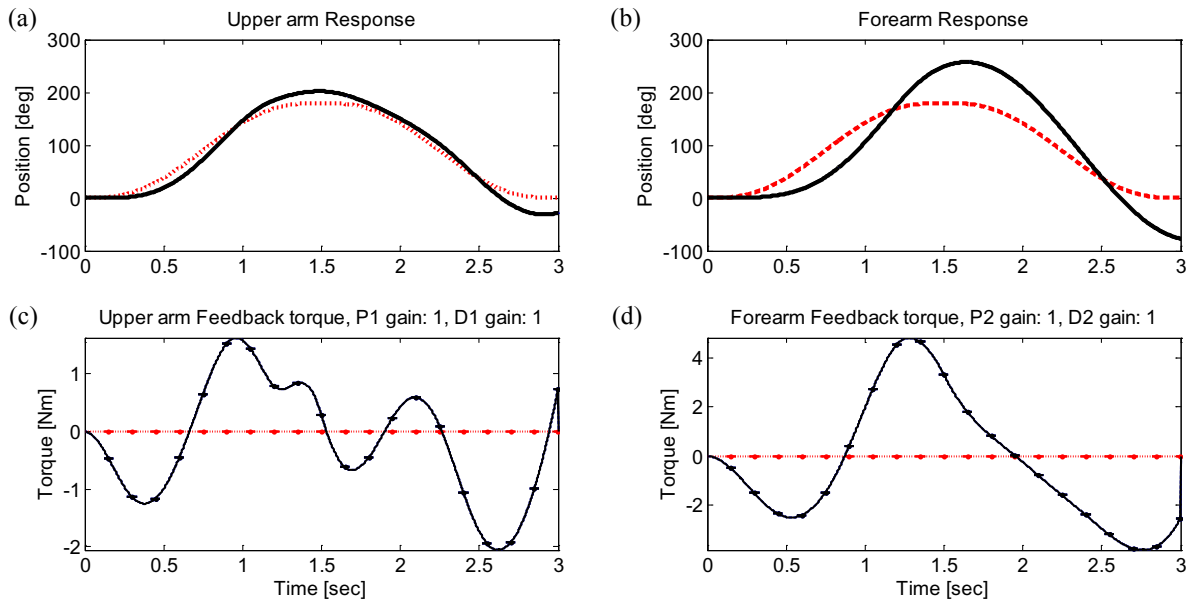
Fig. 4. Computational results using only the PD feedback controller algorithm; (a) & (b) Upper arm and forearm trajectory response, a comparison between the obtained trajectory (solid line), and the desired trajectory (dashed line) set by PCST; (c) & (d) Torque produced by the PD feedback controller at the upper arm & forearm in order to achieve the desired trajectory. The feedback controller gains were all set at 1.

Based on the results, it can be seen that no adaptive control or learning of the necessary torque to achieve the desired task trajectory by only using the conventional PD feedback controller, even though repetitive trials were carried out. Nevertheless, the control properties can only be achieved by manual tuning of the PD controller gains by using various tuning methods such as the Ziegler-Nichols method or by just trial-and-error approach. However, although this type of controller is widely used in the field of robotics [22], implementing this type of control strategy is not practical to model human control. This is because, the manual tuning of the PD controller gains would require exhaustive computational time in searching the optimal values for the gains to achieve the desired trajectory, and also would be harmful to the patient if during the learning process, inadequate torque is exerted by the controller that could damage the patient's arm rather than improving them. Apart from that, fast, smooth and coordinated arm movements cannot be executed by just depending solely on feedback control [23].

3.2. PCST with PD feedback and feedforward controller

Adding a feedforward control into the existing PD feedback control algorithm improves the performance of the 2-DOF system in executing the PCST task, as shown in Fig. 5 and Fig. 6.
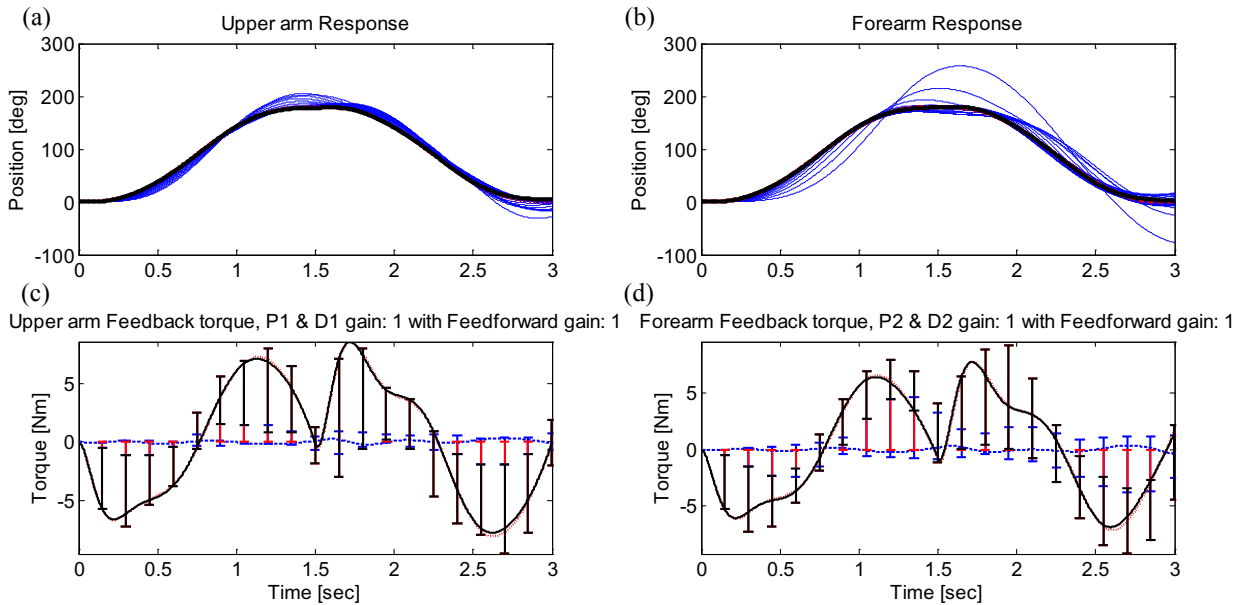

Fig. 5. Computational results using the combined PD feedback and feedforward controllers algorithm; (a) & (b) Upper arm and forearm trajectory response, a comparison between the obtained trajectory (solid line), and the desired trajectory (dashed line) set by PCST, after 30 number of trials. It can be seen that the desired trajectory is obtained after the task is repeated for a number of trials, due to the overlapping of lines between the final trial obtained and desired trajectories; (c) & (d) Torques produced by the PD feedback controller (dashed line), feedforward controller (dotted lines) and the total learnt torque (solid line) with error bars, at the upper arm & forearm. The feedback and feedforward controller gains were all set at 1. As the number of trials increases, the amount of feedback torque produced decreases and is fed into the system as feedforward torque.

After 30 repeated trials of the PCST task, the algorithm learns the desired trajectory by taking the information of the necessary torque required from the feedback controller, and feeding it into the system as a feedforward torque by a gain value, α, in the subsequent trial. The advantage of this control strategy is that the algorithm pre-emptively identifies the amount of torque that is necessary to execute the designated task. This is the learning aspect of the algorithm, which is consistent of the human control strategy known as Feedback Error Learning (FEL), where a human learns from previous 'mistakes' in order not to repeat them again in subsequent similar tasks.
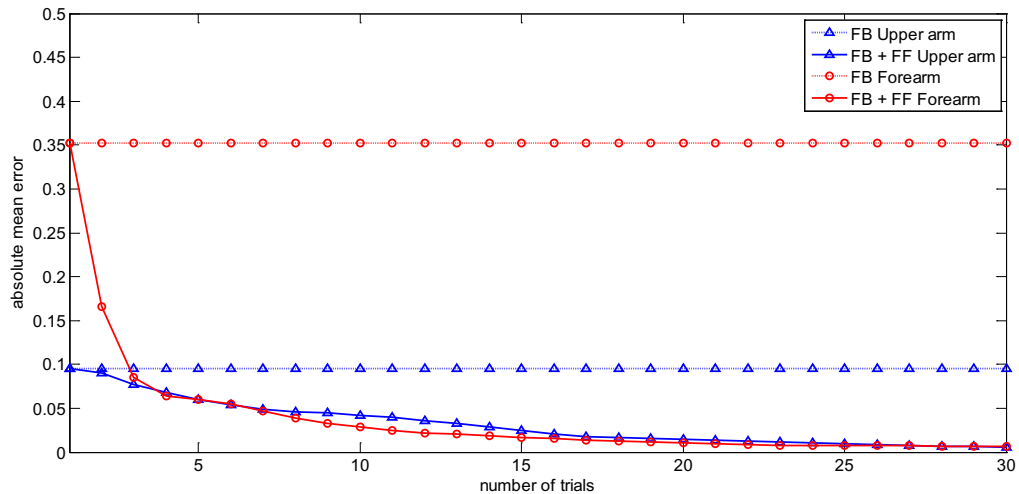
Fig. 6. A comparison between error progressions when both controllers (feedback control and Feedback Error Learning (FEL) control strategy) are used in the algorithm for the same PCST task repeated for 30 trials. The feedback control (using only PD controller) shows no sign of error decrement throughout the 'exercise session', whereas for the combination of feedback and feedforward controller shows a decrement of error for both upper arm and forearm at the end of the simulation. The initial absolute mean errors for both upper arm and forearm during the first trial were 0.0953 and 0.3526 respectively. As the exercise progressed after 30 trials, the absolute mean error were 0.005859 and 0.006138, which is a 93.9% and 98.2% decrement in error response for both upper arm and forearm. This shows that the algorithm exhibited learning and adaptive properties in order to achieve the objective in performing the desired PCST task.

4. Conclusion and Future Work

A computational model of human motor control based on Feedback Error Learning (FEL), as an adaptive algorithm for a nonlinear 2-DOF arm model was successfully developed, simulated and tested in MATLAB® software. A distinct feature in this algorithm is the 2-DOF mathematical model that is used as the core element. The approach of using the mathematical concepts, Lagrangian and Euler-Lagrange equation; in achieving the dynamic equation to mimic the upper arm and forearm segments of the human arm is unique and versatile in developing this algorithm.

Apart from that is also the ability for the algorithm to learn and adapt its trajectory in order to achieve the desired task objective, in contrast of having to manually adjust and update the controller gain parameters. Thus, the algorithm managed to exhibit humanlike properties when executing tasks, assisting researchers in further understanding the adaptive properties and human motor control strategies. Based on the computational results shown in Fig. 5, the torque required to control the 2-DOF limbs range between ±7Nm, depending on the application of the controller. Even though, this algorithm is designed to suit the human upper arm and forearm, nevertheless the algorithm can also be implemented to other applications such as robotic finger rehabilitation device [24].

However, in order to improve on the algorithm before implementing it on an actual robot, thus strengthening the obtained outcomes of this study via experimental results; the stability analysis of the parameters for the controller gains needs to be carried out in the next stage of this study. Given the system modelled in this study is time-variant; therefore the standard transfer function that relates the input-output relationship is not able to be determined. The range of convergence of the parameters used can be obtained by using alternative control analysis methods that are not presented in this paper.

References

[1] Antonio F, Caterina P, Carmelo C, Ilaria C, Luca B, Massimo B, Bruno R, Maria CC. Positive effects of robotic exoskeleton training of upper arm limb reaching movements after stroke. Journal of NeuroEngineering and Rehabilitation 201. p.;9:36

[2] Nancy GK, Rebecca Z, Andrew JB, Steven LW, Jay LA. Quality-of-life change associated with robotic-assisted therapy to improve hand motor function in patients with subacute stroke: a randomize clinical trial. Physical Therapy 2010;90(4). p. 493-504

[3] Hermano IK, Mark F, Stephen PB, Miranda JN, Antonio M, Michael S, Daniel L, Bruce TV, Neville H. Rehabilitation robotics: pilot trial of a spatial extension for MIT-Manus. Journal of NeuroEngineering and Rehabilitation 2014.

[4] Andrade, A. O., Pereira, A. A., Walter, S., Almeida, R., Loureiro, R., Compagna, D., & Kyberd, P. J. Bridging the gap between robotic technology and health care. Biomedical Signal Processing and Control, 2014;10:65-78.

[5] Kohler, F., Schmitz-Rode, T., & Disselhorst-Klug, C. Introducing a feedback training system for guided home rehabilitation. Journal of neuroengineering and rehabilitation, 2010;7(1):2-11.

[6] Ricardo A, Hassan KA, Mostafa S. A generalized fractional variational problem depending on indefinite integrals: Euler–Lagrange equation and numerical solution. Journal of Vibration and Control 2013;19(14):2177-2186.

[7] Dongling W, Aiguo X. Fractional variational integrators for fractional Euler–Lagrange equations with holonomic constraints. Communications in Nonlinear Science and Numerical Simulation 2013;18(4):905-14.

[8] Jose AV. Euler–Lagrange equations for functionals defined on fréchet manifolds. Journal of Nonlinear Mathematical Physics 2009;16(4):443-454.

[9] Chapra SC, Canale RP. Numerical methods for engineers. 6th ed. McGraw-Hill International edition; 2010, pp. 708-26.

[10] Ogata K. Modern control engineering. 5th ed. Pearson International edition; 2010. pp. 577-86

[11] Etienne B. Signals, systems and control. Biomedical Engineering Department, Imperial College London, UK 2007. p. 38

[12] Qiang Z, Shu-Rong L, Xiao-Shan G. Practical smooth minimum time trajectory planning for path following robotic manipulators. IEEE American Control Conference (ACC) 2013. p. 2778-83

[13] Alexander Y, Ke Z, Yusuf A. Smooth trajectory generation for five-axis machine tools. International Journal of Machine Tools and Manufacture 2013;71:11-9.

[14] Witelski T, Virgin LN, George C. A driven system of impacting pendulums: Experiments and simulations. Journal of Sound and Vibration 2014;333(6):1734-53.

[15] Sanyal AK, Goswami A, dynamics and balance control of the reaction mass pendulum: a three-dimensional multibody pendulum with variable body inertia. Journal of Dynamic Systems, Measurement, and Control 2014;136(2):021002.

[16] Hibbeler RC. Mechanics of Materials. 8th ed in SI units Pearson Prentice Hall; 2011: p. 304-5.

[17] Hibbeler RC. Mechanics of Materials. 8th ed in SI units Pearson Prentice Hall; 2011: p. 787-8.

[18] Etienne B, Gowrishankar G, Yang C, Alin AS. Interaction force, impedance and trajectory adaptation: by humans, for robots. Experimental Robotics, Springer Berlin Heidelberg 2014: p. 331-45.

[19] Flash T., & Hogan, N. The coordination of arm movements: an experimentally confirmed mathematical model. The journal of Neuroscience, 1985; 5(7):1688-1703.

[20] Subramaniam P, Arif WO, Velappa G. Development of robot assisted stroke rehabilitation system of human upper limb. IEEE Automation Science and Engineering 2009. pp. 256-61.

[21] Etienne B, Codourey A, Rey L. Experimental evaluation of nonlinear adaptive controllers. IEEE Control Systems Magazine 1998;18(2):39-47.

[22] Huang J, Yang, C., & Ye, J. Nonlinear PD Controllers with Gravity Compensation for Robot Manipulators. Cybernetics and Information Technologies 2014;14(1):141-50.

[23] Armendariz J, Parra-Vega V, Garcia R, Shinichi H. Dynamic self-tuning PD control for tracking of robot manipulators. 51st IEEEConference on Decision and Control 2012. p. 1172-1179.

[24] Low C, M.A.A. Kasim, T. Koch, R. Dumitrescu, H. Yussof, R. Jaafar, A. Jaffar, A. Aqilah, K. Ng. Hybrid-Actuated Finger Prosthesis with Tactile Sensing. International Journal of Advanced Robotic Systems: Smart Sensors for Smart Robots 2013;10:351-61.